

A Design of Experiments Approach Towards Desired Flow Distribution Through Manifolds in Electronics Cooling

Annappurna Sogunuru,^{#,*} Suma Varughese,[#] A.C. Niranjanappa,[#] and K. Hemachandra Reddy[§]

DRDO - Centre for Airborne Systems (CABS), India

[§]JNTU College of Engineering, Anantapur, India

**E-mail: annappurna.cabs@gov.in*

ABSTRACT

For rack-mounted electronics, flow distribution is desired as per the heat load characteristics. In the literature, attainment of flow uniformity through manifolds is highlighted and widely discussed as it has more applications. To attain desired flow distribution, the complexity of the problem increases. In the present paper, the Design of Experiments (DOE) along with response surface optimization is used to arrive at desired flow, which includes uniform flow also. A three-dimension, 10-channel Z-type manifold is considered for the study. This model is taken from experimentally verified and published data for which desired flow patterns are achieved. Flow requirement through each channel is set as a parameter for optimization and by the defined sample set under DOE, uniform flow and pattern flow are achieved by introducing suitable orifices. Multi-Objective Genetic Algorithm (MOGA) is used for obtaining orifice diameters. A good agreement is observed between the attained flow patterns and desired patterns. This approach is simple and can be implemented for industrial applications.

Keywords: Manifold; Flow distribution; DOE; MOGA

NOMENCLATURE

a	Cross-sectional area of orifice, m ²
C _d	Orifice coefficient of discharge
d	Orifice diameter, m
D	Branch channel diameter, m
f	Limiting factorial number
k	Number of input parameters
\dot{m}_a	Attained mass flow rate, kg/s
\dot{m}_d	Desired mass flow rate, kg/s
n	Number of channels
p	Static pressure of the fluid, Pa
Q	Water flow rate, m ³ /s
\bar{v}	Velocity of fluid, m/s
\dot{V}	Volume flow rate, m ³ /s
ρ	Density of the fluid, kg/m ³
μ	Viscosity of the fluid, Pa.s
x	Design variable

ABBREVIATIONS

DF	Deviation Factor
DI	Deviation Index for mass flow rate
DoE	Design of Experiments
HVAC	Heating, Ventilating, Air Conditioning
LRU	Line Replaceable Unit
MOGA	Multi-Objective Genetic Algorithm

SUBSCRIPTS

a	attained
d	desired
f	final
i	initial
L	lower bound
m	mass flow rate
U	upper bound

1. INTRODUCTION

Flow distribution through manifolds has applications in electronics cooling¹⁻⁴, HVAC systems^{5,6}, heat exchangers⁷⁻¹¹ boilers¹², nuclear reactors¹³⁻¹⁴, heat transfer applications¹⁵⁻¹⁶, solar collectors equipment¹⁷, chemical processing fuel cells,¹⁸ etc. Being enriched with vast research for the past few decades, still this topic has scope for further investigation as the applications are varying day by day.

A manifold is a fluid flow chamber that either divides the flow from a single inlet to numerous exits or combines the flow from numerous exits to a single outlet. When the fluid gets distributed from a single inlet line, it is called a distribution header. When the fluid converges to a single outlet line, it is called a collection header. The numerous branches connected to these single lines are called channels. Widely used manifold configurations are shown in Fig. 1^{1,11,19}. There are several other types also, which are application dependent⁵⁻⁷.

Flow distribution inside the manifolds depends upon the associated geometry friction losses, turning losses, the transition of pressure, and momentum inside the headers. Pressure drops across the channel drive fluid flow through it. These factors are configuration dependent and are unique to each type of manifold system.

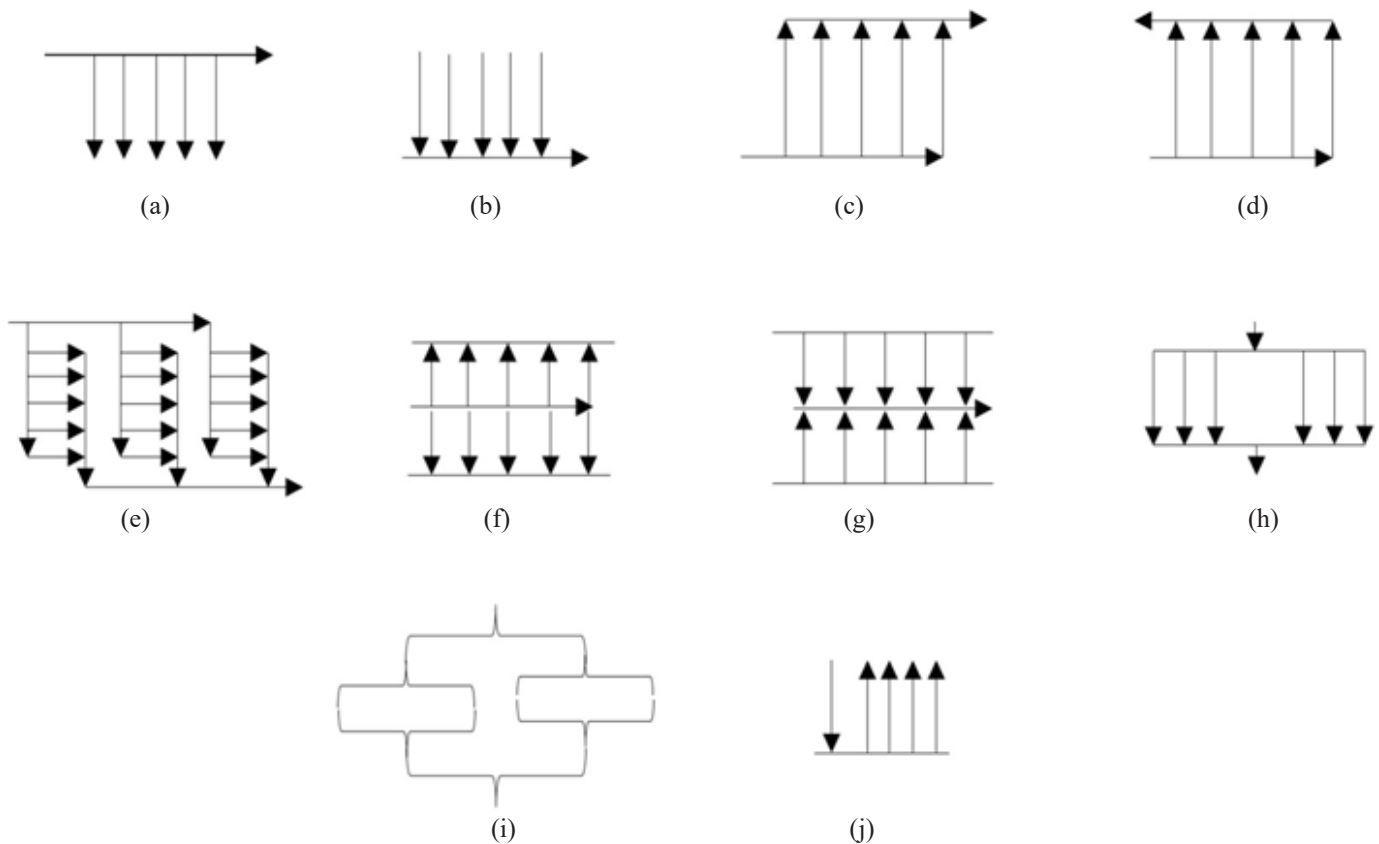


Figure 1. Different type of manifold configurations (a) Dividing, (b) Combining, (c) Z-type, (d) U-type, (e) Nested, (f) Central feed dual out, (g) Dual in central out, (h) Split and combine flow, (i) Bifurcation and (j) Parallel.

Reasons for maldistribution inside the manifolds were studied extensively by several researchers. Gandhi,⁷ *et al.* have summarized some of the major contributions in chronological order. Wang,^{19,20} *et al.* have discussed analytical and discrete approaches²¹ for finding solutions to manifold problems. In the available literature, the complexity of flow distribution through manifolds is reduced by the following assumptions: (i) all the channels are uniformly spaced (ii) flow across all the channels is the same and (iii) all channels have the same cross-sectional area. With the advent of Computational Fluid Dynamics (CFD) software, conjugate heat transfer problems are also being solved. Since applications of flow uniformity are wider, and maldistribution is considered an unequal distribution, it has been extensively discussed in the literature. Flow uniformity across the channels is declared as the key performance evaluator in the manifold distribution systems¹⁻¹⁸.

Wei^{22,23}, *et al.* and Zeng²⁴, *et al.* have identified that in applications like solar tubular receivers, and heat exchangers, non-uniform but desired flow distribution is required. Hence, flow maldistribution is re-defined as the deviation from the target or desired distribution. To attain desired flow, Wei, *et al.* developed a CFD-based algorithm. They analysed a 2D model of 15 channels between distribution and collection manifolds with middle inlet-outlet and diagonal inlet-outlet configurations. In their study, a perforated baffle plate is inserted in the distribution manifold and orifice diameters are iteratively controlled by the error between target flow rates and flow rates from the previous

iteration for each channel. Zeng, *et al.* have performed multi-stage topology optimization on a 2D model with middle inlet and outlet configuration of the manifolds to achieve target flow distribution. In both studies, desired flow distribution is attained by the geometry modification of the inlet manifolds. However, it may not always be feasible to make geometry modifications to achieve the desired flow pattern, as this issue needs to be addressed at the design level. Hence an alternate approach is sought.

In airborne applications, avionic (electronic) racks are very compact due to weight and space constraints. These electronic racks typically consist of several Line Replaceable Units (LRUs) arranged in tandem. In this, coolant is distributed to cold plates using manifolds. LRUs are butted to the cold plates. All the rack-mounted LRUs always may not have similar heat loads. Sometimes, though the LRU configuration is the same, heat loads may vary as per the operating duty cycle. Hence, flow uniformity across all coolant channels in the racks may not be always desirable.

Sogunuru⁴, *et al.* proposed a numerical approach to meet the pattern flow requirement for a 10-channel Z-manifold configuration. In their study, the pressure drop that drives desired flow through each channel is calculated using the Hagen-Poiseuille equation. For each channel, the corresponding pressure drop obtained from CFD simulations is compared. For each difference in pressure drop, orifice sizes are calculated by solving the following orifice equation:

$$Q = \frac{C_d a \sqrt{2 \nabla p}}{\sqrt{\rho(1 - \beta^4)}} \quad (1)$$

where, $\beta = d/D$

After obtaining a set of orifice diameters, CFD simulations are performed. Simulations are continued with the modified orifice diameters, after each iteration, to reduce the deviation to an acceptable level. However, in this approach, except for the numerical simulations, every step needs manual intervention, which is a cumbersome exercise. Also, for channels of varying cross-sections, theoretical calculation of pressure drop that drives desired flow is not possible. Hence an alternate, easy method is required. To the authors' knowledge, in the available open literature, a simple approach to attain desired flow pattern using DoE techniques in the manifold system could not be found.

In the manifold system, flow across each channel is affected by the flow across other channels. To achieve desired flow through each channel, each channel needs a flow control valve or a suitable orifice. Hence, considering the orifice diameter of each channel as an input parameter, the influence of all the parameters can be studied simultaneously to obtain desired flow through each one of them. This becomes a multi-parameter and multi-objective function problem. Hence, the Design of Experiments approach can be used to achieve desired flow distribution. The following three configurations are considered for the present study.

1. Uniform flow
2. Flow Pattern -1
3. Flow Pattern -2

The flow pattern-1 and flow pattern-2 of the Z-configuration manifold are studied by Sogunuru⁴, *et al.* and are chosen for the present paper as they are validated experimentally.

2. DESIGN OF EXPERIMENTS (DOE)

DOE is a scientific approach in which a series of experiments are conducted for a given set of parameters within a specified range that minimizes the number of runs needed to understand the influence of parameters. Figure 2 shows a typical framework²⁵ of DOE for a system or a process.

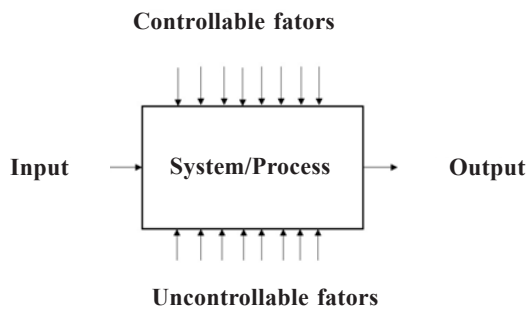


Figure 2. General framework of DoE for process/system.

To get a better output response, a greater number of samples are required to conduct more experiments. However, this is an intensive exercise. From a smaller number of samples, the desired results may not be achieved. Hence choosing an

appropriate and a minimum number of samples that can have maximum influence on the output response is very essential for conducting the experiments.

The number of samples generation to conduct experiments depends on the selection of DoE schemes²⁶⁻²⁹. The Central Composite Design and Box Behnken Design schemes are categorized as classical or black box sampling schemes because the objective function need not be known a priori. These schemes are robust and use second-order designs to fit full quadratic objective functions²⁹.

In Central Composite Design, each input parameter is divided into three or five levels between its maximum and minimum values. It uses central points, extreme or corner points, and either face points or extended points. Central composite designs with face points require three levels. With extended axial points called star points, five levels are required. In Box Behnken Design, the input parameter is divided into three levels and hence the number of generated samples will be less. So, predictive accuracy levels are less compared to central composite design. Figure 3 shows the spread of points in the Central composite design for two and three variables.²⁶

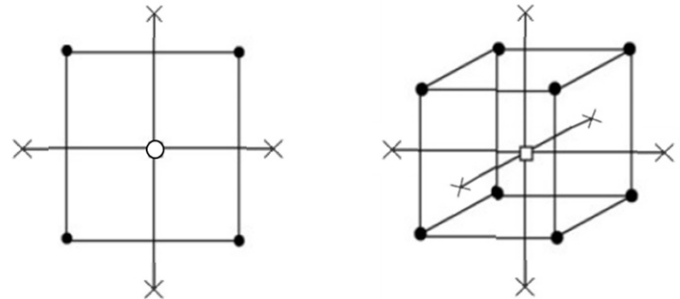


Figure 3. Central composite design for two variables (left), three variables (right).

To reduce the number of experimental runs, and for more accuracy levels, optimal designs are available. These are called white-box functions since the objective function is known a priori²⁹. Optimal Space Filling Design, Sparse Grid Design, and Latin Hypercube Sampling Design are a few optimal designs. In Optimal Space Filling Design each input parameter is divided into several parts to achieve the maximum analytical vision using the least number of points. In the Sparse Grid method, each input parameter is divided into three levels, however in this, when the gradient in the desired output parameters is more, the matrix of the design points can be corrected to increase the accuracy levels of the response level. The Latin Hyper Cube Sampling uses the Monte Carlo sampling method and the design points are randomly generated with a maximum possible spread in the design space. Several research papers are available detailing each model. However, the selection of the appropriate scheme for DoE requires adequate engineering knowledge.

The DoE generates the data for output parameters corresponding to the design points based on the selection of the DoE scheme. To know the continuous variation of the performance output parameter over a given variation of the input parameter, a Meta model or a response surface is used. Response surface is a simple approximation to a computationally

intensive function,²⁸ that is the best fit surface through the calculated points to the interpolated space. It provides the approximated values of the output parameters corresponding to the input parameters everywhere in the analyzed design space, without the need to perform a complete solution. The interpolation spaces can be generated by different methods like second-order polynomial, Kriging, neural networks, sparse grid methods, non-parametric regression, etc.

With a sufficient number of design points and a good spread across the sampling space and with appropriate interpolation methods, an optimal solution that meets the required objectives is obtained.

A standard non-linear optimization problem is usually formulated²⁸ as

$$\begin{aligned}
 &Max / Min F(x) \\
 &S.T. g_k(x) \leq 0, (k = 1 \dots K) \\
 &x \in [x_L, x_U]
 \end{aligned}
 \tag{2}$$

where, $x = [x_1, x_2, \dots, x_n]^T$ is a vector of design variable; x_L, x_U are the lower and upper bounds vectors, respectively, which define the search range for each factor, and together define the design space.

In the present work, the Z-manifold is the system considered as explained in Fig. 2. Input is the mass flow rate through the inlet and output is the desired flow rate through each channel. Controllable factors are the orifice diameters and the uncontrollable factors are the geometry and the pressure losses associated with it. This defines the problem. An optimal solution is the one that gives the desired flow with minimum pressure loss for the overall configuration. Figure 4 provides the methodology of DoE with the optimization process adopted in the present study in the form of a flow chart.

3. CFD MODEL

A Z-type manifold geometry is created in the ANSYS Design Modeler. The bottom inlet and top outlet are considered. Diameters of header and channel are taken as 12 mm and 6.5 mm respectively. Ten channels are considered with a pitch of 70mm. The total length of the manifold considered is 700 mm. The total height of each channel is 440 mm. Since orifice diameter is a variable factor for each channel to be optimized, a length of 20 mm at the mid-portion of a total 440 mm channel height is modeled separately in Design Modeler and defined as a parameter. Figure 5 shows the schematic of the Z-manifold with dimensions. In this, d_1 to d_{10} represents the orifice diameters which are defined as input parameters.

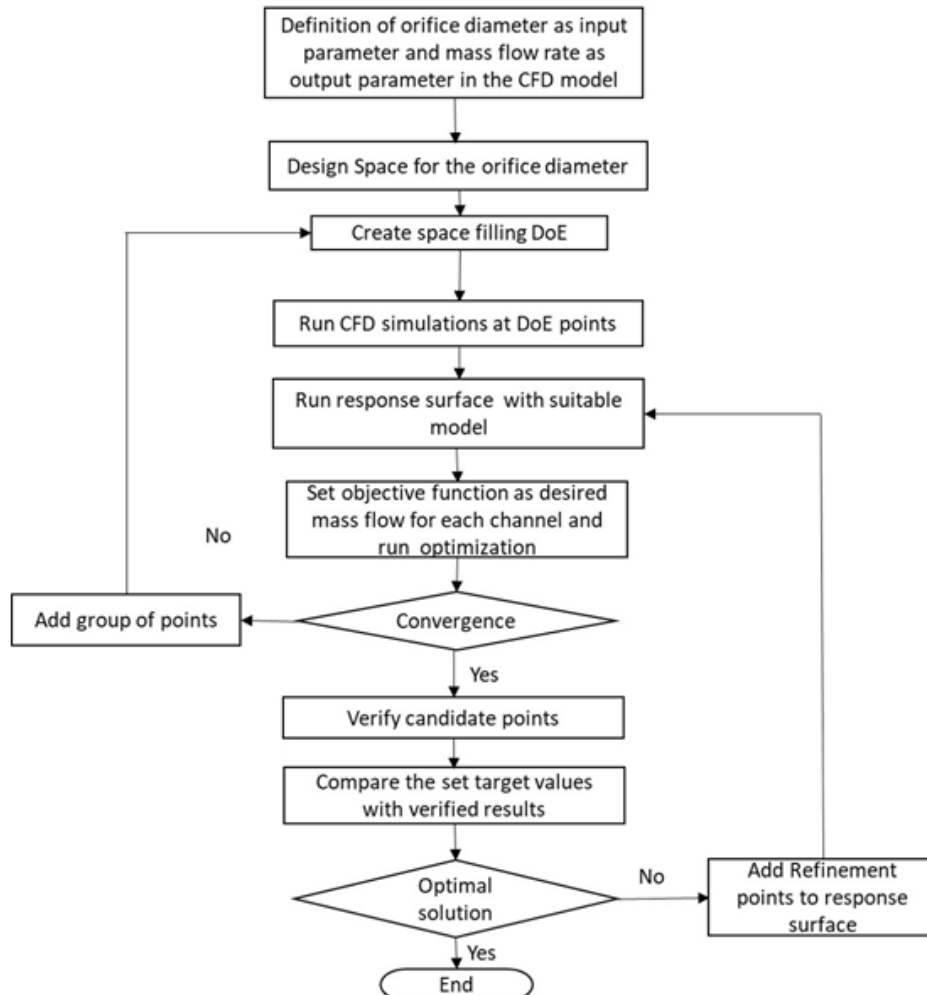


Figure 4. Flow chart of DoE with response surface optimization.

For 10 channels, 10 parameters are defined. Numerical mesh is prepared in ANSYS ICEM-CFD. Hex dominant mesh is used for the overall computational domain to have quality mesh. The multi-Zone method is used to generate the fine mesh at the orifice portions. In the vicinity of the junctions, a few tetrahedral elements are used instead of the dominant hexahedral cells to capture the fluid properties accurately at the junctions of the manifolds. The fine mesh used is of 0.001mm element size. The average element quality is maintained at 0.7. Fig. 6 indicates mesh for the fluid domain of the 3D manifold configuration investigated in the present study. At the inlet of the distribution header, the velocity inlet boundary condition is applied. At the outlet of the collection header, a pressure boundary condition is applied. At the closed end of both the headers, wall boundary conditions are considered.

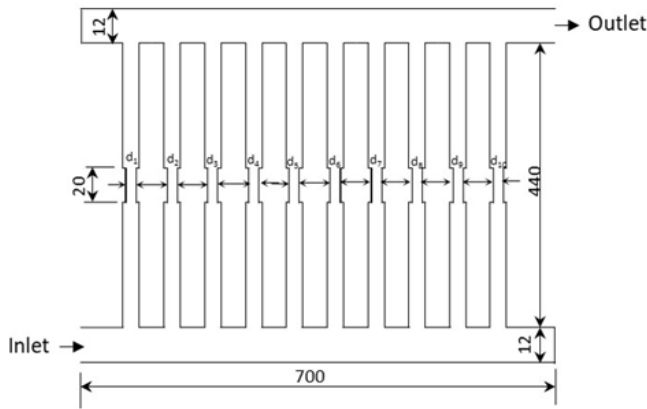


Figure 5. Schematic of Z-manifold system considered for numerical simulations.

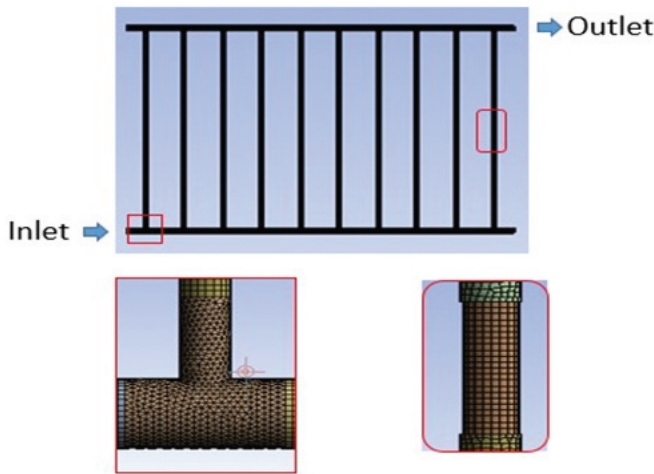


Figure 6. Model and mesh considered for numerical simulations.

4. SOLUTION METHODOLOGY AND CFD SIMULATIONS

ANSYS Fluent 19.2 is used for CFD simulations. The flow-through manifold distribution system is considered incompressible, of constant viscosity, and steady. Gravity forces are neglected. Fluid is selected as Water with a density of 998 kg/m³ and dynamic viscosity of 0.00089 Pa.s.

The mass conservation equation used for solving is as follows:

$$\nabla \cdot \vec{v} = 0 \tag{3}$$

The momentum conservation equation used for solving is written as follows:

$$(\vec{v} \cdot \nabla) \vec{v} = -\frac{1}{\rho} \nabla p + \frac{\mu}{\rho} \nabla^2 \vec{v} \tag{4}$$

where \vec{v} is velocity, p is static pressure, ρ is the density of the fluid.

Pressure-velocity coupled; the second-order upwind scheme is chosen as the solution method. This method obtains a robust and efficient performance for steady-state single-phase flows, and solves momentum and pressure-based continuity equation together.

Initial configuration is analyzed first for 6.5mm diameter throughout the channel length and the flow rates across each channel are noted. This is considered the Natural flow configuration.

The initial mesh has 4,53,000 cell numbers. It is refined successively thrice by a refinement factor of 1.5. Iterations are carried out for the residuals of five orders of magnitude for each case. Mass flow rates across each channel are compared for each case. Results are checked for grid independence. Mesh with a cell number of approximately about 10, 20,000 is finalized with negligible deviation in mass flow rates in successive iterations. As indicated in Fig. 5, each channel orifice diameter is independently defined as an input parameter and the mass flow rate across each of them is defined as output parameters corresponding to it. The Central Composite method is chosen as the DoE scheme due to its robustness. For each input parameter, Lower and upper bounds are defined as 1mm and 6.5mm respectively. The number of the sample points generated in the ANSYS Workbench for 10 input parameters is 149. This is calculated automatically using the formula $2^{(k-f)} + 2k + 1$. In this k is the number of input parameters which is equal to 10. f value is 3. f is the limiting factor corresponding to 10 input parameters. Hence the number of generated samples is 149.

To generate the Response Surface, the Genetic Aggregation (GA) method is chosen with an option to generate rectification points in the Workbench. Desired flow through each channel is set as the objective function before running the optimization scheme. For the same DoE samples, three optimization cases are run separately to achieve the three desired flow patterns. The multi-Objective Genetic Algorithm (MOGA) is selected to obtain global optimum values for all three cases. Generated candidate points are verified against the desired flow.

Simulations are performed in an AMD Ryzen™ 9 4900HS, a 64-bit system having an eight-core processor with 16 threads and 16.00GB RAM. Each optimization simulation is converged after 11958 evaluations.

To compare the distribution between the desired and attained flows, a dimensionless Deviation Index (DI_m) is introduced, which is defined as:

$$DI_m = \left(\frac{m_a - m_d}{m_d} \right) * 100 \tag{6}$$

where, \dot{m}_a is the mass flow rate attained, and \dot{m}_d is the desired mass flow rate.

To reduce DI_m to a reasonable level, verified candidate points are inserted as refinement points. On the modification of the Response Surface, Optimization is carried out to get the desired flow to the level of acceptable accuracy.

Another dimensionless number DI_d is introduced that provides the deviation from the initial diameter (d_i) of the channel which is 6.5mm.

$$DI_d = \left(\frac{d_i - d_f}{d_i} \right) \tag{6}$$

5. SENSITIVITY ANALYSIS

The purpose of carrying out sensitivity analysis is to understand the influence of the design variables or the input parameters on the output or performance of the object. By doing so, more attention can be paid to optimising the key influencing factors that save computational time. However, variation of one variable at a time may not provide a complete idea of the overall structure of the problem as in the present case. In such conditions, the response surface approach provides good insight into the design problem.

Figure 7 presents the local sensitivity diagram obtained from the ANSYS Workbench for the present manifold configuration, in terms of a bar chart for natural flow configuration. Indicated on the top right of this figure, P1 to P10 are the input parameters. These are the orifice diameters of all the 10 channels. On the x-axis, the indicated parameters P11 to P20 are the mass flow rates across the channels from channel 1 to channel 10. From this figure, it is evident that each channel output parameter is highly influenced by the respective channel diameter. And the effect of orifice diameters of the last five channels is predominant when compared to the effect of orifice diameters of the first five channels.

6. RESULTS AND DISCUSSION

6.1 Natural and Uniform Flow

For the natural flow configuration, the mass flow rate is more towards the last few channels, as expected. A section plane is drawn at the middle of the manifold system at the (0,0,0) coordinate and velocity contour plots are taken for all the studied cases. The velocity contour for the natural configuration is shown in Fig. 8. For the objective function of

flow uniformity, the results obtained are plotted in Fig. 9. In the same figure, the mass flow rate across each channel for the natural case is also plotted and compared. The obtained velocity contour plot for uniform flow is presented in Fig. 10.

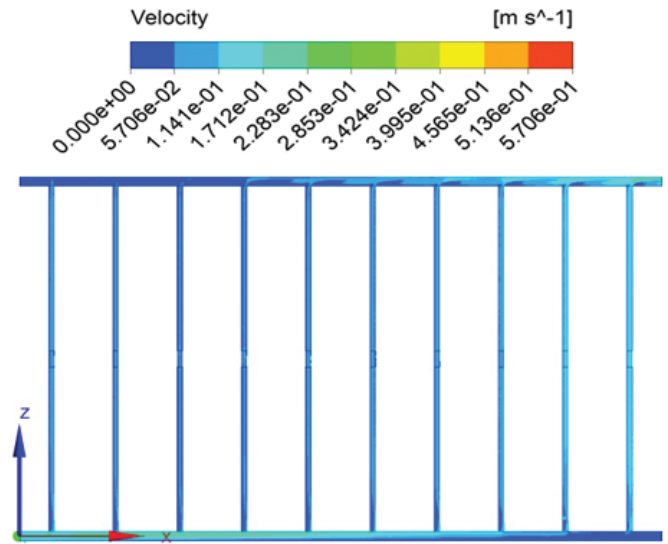


Figure 8. Velocity contour plot for natural flow distribution.

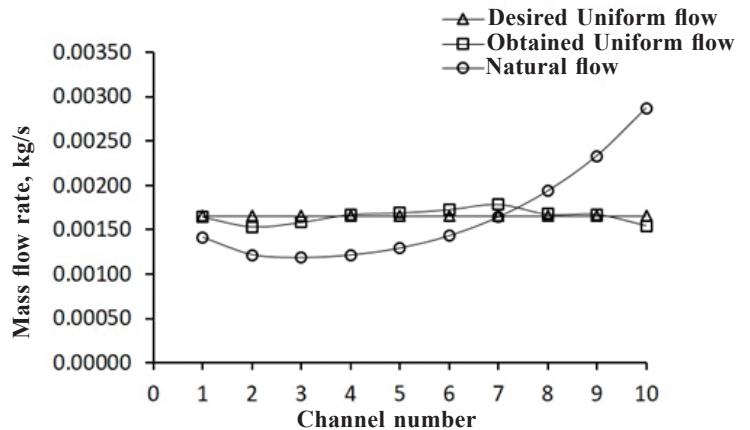


Figure 9. Mass flow distribution across channels for natural and uniform flow cases.

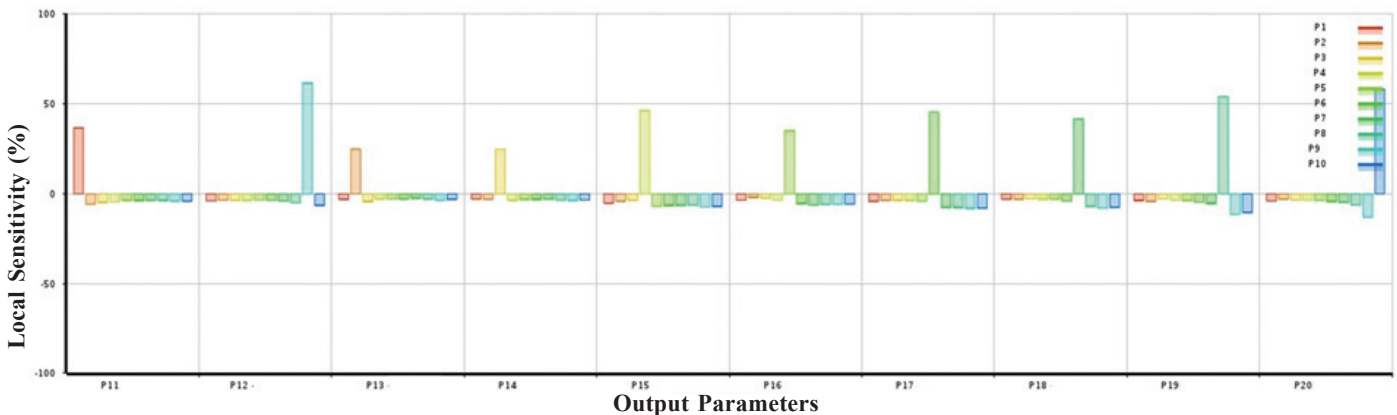


Figure 7. Sensitivity chart obtained from ANSYS workbench for natural flow configuration.

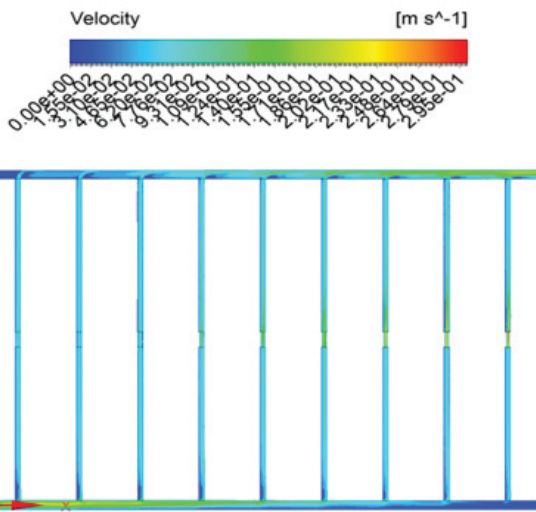


Figure 10. Velocity contour plot for uniform flow distribution.

6.2 Flow Pattern-1

The desired flow Pattern-1 configuration and attained mass flow from the CFD simulations are compared and shown in Fig. 11.

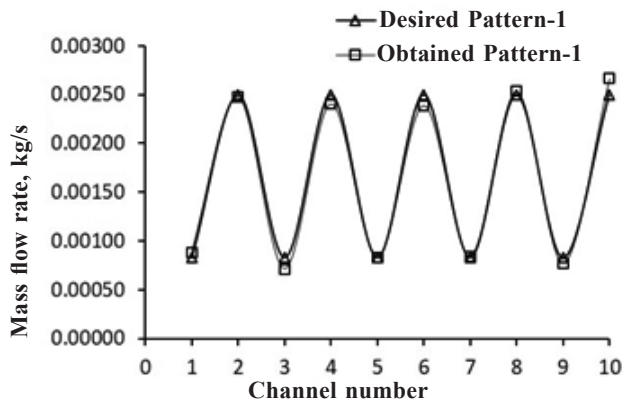


Figure 11. Mass flow distribution across channels for flow pattern-1.

Figure 12 shows the velocity contour plot for this flow pattern.

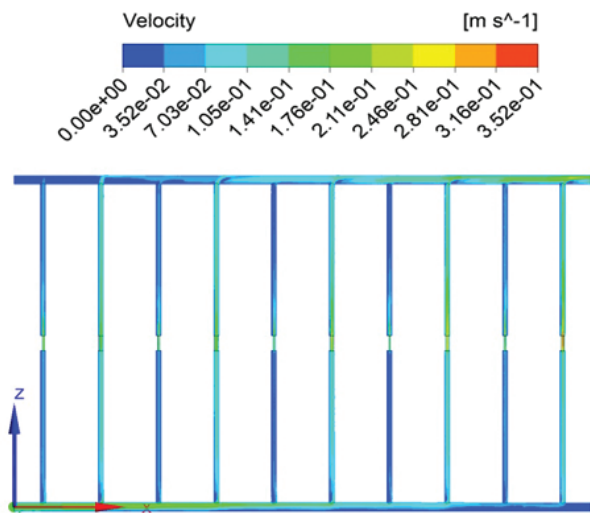


Figure 12. Velocity contour plot for flow pattern-1.

6.3 Flow Pattern-2

The desired flow and achieved mass flow across each channel for Pattern-2 are compared and presented in Fig. 13. The velocity contour plot corresponding to this pattern is shown in Fig. 14.

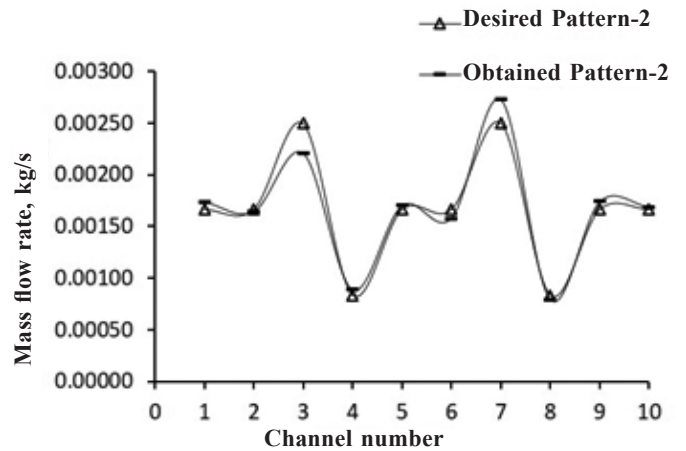


Figure 13. Mass flow distribution across channels for flow pattern-2.

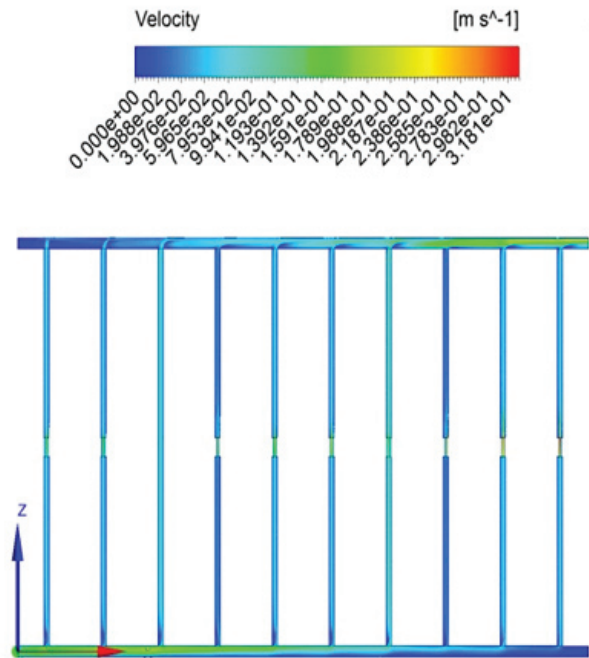


Figure 14. Velocity contour plot for flow pattern-2.

The dimensionless Deviation Index for each studied pattern is plotted and compared as shown in Fig. 15. In this, positive values on the y-axis indicate excess low and negative values indicate short flow. For Natural flow, DI_m is calculated for the values of Uniform flow. It is seen in this figure that, DI_m for Natural flow is in the range of -28.4 to +73.6. This is reduced to -7.3 to 8.4 for Uniform flow. For optimized flow Pattern-1, DI_m lies in the range of -14.4 to +6.9. Similarly, optimized flow Pattern-2, DI_m lies in the range of -14.6 to 9.

For each type of flow, the Deviation Factor as defined by Wei *et.al.*²², is calculated using the formula

$$DF = \sqrt{\frac{1}{(n-1)} \sum_{i=1}^n \left(\frac{\dot{m}_{attained}}{\dot{m}_{desired}} - 1 \right)^2} \quad (7)$$

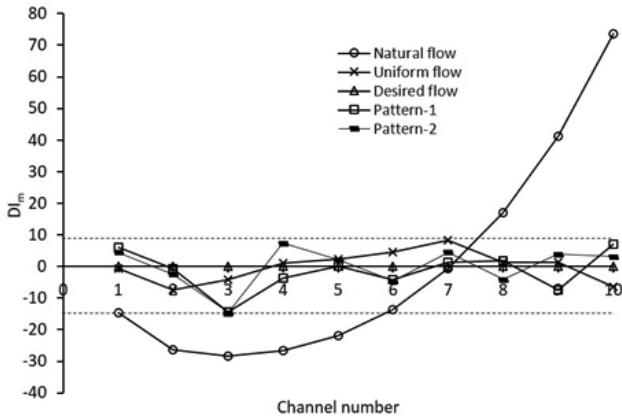


Figure 15. Channel wise DI_m for all the studied cases.

Total Pressure drop for all the cases and DF values are presented in Table 1. It is seen from the table that for the uniform flow, DF is the maximum. As predicted, the maximum pressure drop is observed for flow Pattern-1 case. This is because, to attain peak minimum flow for every alternate channel, orifice diameters are reduced, and accordingly pressure drop increases.

DI_d for the Uniform flow, flow Pattern-1 and flow Pattern-2 cases are plotted for each channel as shown in Fig. 16. It is interesting to observe that the trend of the diameter deviation graphs is opposite to that of the desired patterns.

Table 1. Pressure drop and DF for Analyzed cases

Analyzed case	Pressure drop, pa	DF
Natural flow	60.37162	
Uniform flow	68.50604	0.118
Pattern-1	89.73	0.065
Pattern-2	75.43681	0.065

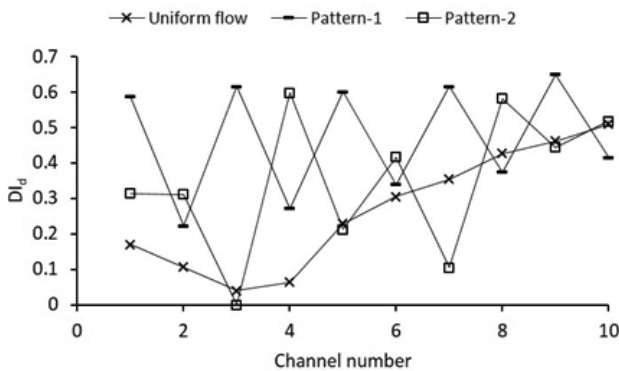


Figure 16. Channel wise DI_d for all the studied cases.

7. CONCLUSIONS AND FUTURE SCOPE

The applicability of DOE techniques to attain three different desired flow patterns in the manifold system is investigated. Results of attained individual channel flow rates for all the investigated patterns are compared with that of the

desired flow rates. A dimensionless Mass flow index (DI_m) is defined to find the deviation. The highest value of DI_m on the positive side in the case of the Natural flow is 73, which has been brought down to 9 which is the maximum of all three cases. Similarly, the Highest value of DI_m in the case of Natural flow is -28.4, on the negative side, has been brought down to -14.6.

DOE approach can be extended to complex manifold problems to find the orifice diameters. With a more reasonable number of samples, it is possible to get further accurate results. This results in a significant reduction in human intervention in model correction after each iteration. This has potential application in solving similar industrial problems. When the number of channels is more, using a Central Composite method to define the sample space would be computationally intensive. By the selection of appropriate DOE techniques, it can be minimized.

The study will be extended in the future to verify the attainment of desired flow in the case of non-uniform and irregular cross-section channels and turbulent flows

ACKNOWLEDGEMENTS

The authors would like to thank the Director, CABS for supporting the research work.

REFERENCES

- Johnson, Scott T. Analysis of manifold networks for air and liquid flow-through Modular electronics. 17th IEEE Symposium, 2001. 233-244
- Sparrow, Ephraim M.; Tong, Jimmy C.K., Abraham, John P. A Quasi-analytical method for fluid flow in a multi-inlet collection manifold. *J. Fluids Engg.*, 2007, **129**, 579 -586 doi: 10.1115/1.2717620
- Tomomura, Osamu; Tanaka, Shotaro; Noda, Masaru.; Kano, Manabu; Hasebe, Shinji; Hashimoto, Iori. CFD-based optimal design of manifold in plate-fin microdevices. *Chem. Engg. J.*, **101**, 2004, 397-402. doi:10.1016/j.cej.2003.10.022
- Annapurna, Sogunuru; Menon, Yash Krishna; Niranjanappa, A.C. & Reddy, K. Hemachandra. Numerical and experimental investigations on patterned flow distribution through manifolds in electronics cooling. *Int. J. Mech. Production Engg. Res. Dev.*, 2020, **10(2)**, 975-986 doi: 10.24247/ijmperdapr202095
- Subaschandar, G. Sakthivel. Performance improvement of a typical manifold using computational fluid dynamics. *MATEC Web of Conferences*, 2016, **54**, 1-4 doi:10.1051/mateconf/20165411004
- Zhang, et al. Effects of geometric structures on flow uniformity and pressure drop in dividing manifold systems with parallel pipe arrays. *Int. J. Heat and Mass Transfer*, 2018, **127**, 870-881 doi:10.1016/j.ijheatmasstransfer.2018.07.111.
- Gandhi, Mayurkumar S.; Ganguli, Arijit A.; Joshi, Jyeshtharaj B.; Pallipattu, K. Vijayan. CFD simulations for steam distribution in header and tube assemblies. *Chem. Engg. Res. Design*, 2012, **90**, 487-506 doi: 10.1016/j.cherd.2011.08.019

8. Vásquez-Alvarez, E.; Degasperi, F.T.; Morita, L.G.; Gongora-Rubio, M.R. & Giudici, R. Development of a micro-heat exchanger with stacked plates using LTCC technology, *Brazilian J. Chem. Engg.*, 2010, **27**(03), 483 - 497
doi: 10.1590/S0104-66322010000300012
9. Wang, Chi-Chuan; Yang, Kai-Shing; Tsai, Jhong-Syuan & Chen Ing, Youn. Characteristics of flow distribution in compact parallel-flow heat exchangers, Part-I: Typical inlet header, *Appl. therm. Engg.*, 2011, **31**, 3226-3234
doi: 10.1016/j.applthermaleng.2011.06.004
10. Huang, Cheng-Hung & Wang, Chun-Hsien. The design of uniform tube flow rates for Z-type compact parallel-flow heat exchangers, *Int. J. Heat and Mass Transfer*, 2013, **57**, 608–622
doi: 10.1016/j.ijheatmasstransfer.2012.10.058
11. Zhou, Jian; Sun, Zhongning; Ding, Ming; Bian, Haozhi; Zhang, Nan & Meng, Zhaoming. CFD simulation for flow distribution in manifolds of central-type compact parallel-flow heat exchangers. *Appl. Therm. Engg.*, 2017, **127**, 1-23
doi: 10.1016/j.applthermaleng.2017.07.194
12. Bianco, Vincenzo; Szubel, Mateusz; Matras, Beata; Filipowicz, Mariusz; Papis, Karolina & Podlasek, Szymon. CFD analysis and design optimization of an air manifold for a biomass boiler. *Renewable Energy*, 2021, **163**, 2018-2028
doi: 10.1016/j.renene.2020.10.107
13. Quintanar, Nicolas R.; Nguyen, Thien, Vaghetto, Rodolfo & Hassan, Yassin A. . Natural circulation flow distribution within a multi-branch manifold. *Int. J. Heat and Mass Transfer*, 2019, **135**, 1-15
doi: 10.1016/j.ijheatmasstransfer.2019.01.102
14. Budiman, Arif Adtyas; Haryanto, Dedy; Muhammad, Subekti & Kusuma, Mukhsinun Hadi. Preliminary study on fluid dynamics in manifolds of the reactor cavity cooling system – The experimental power reactor test facility-symposium of emerging nuclear technology and engineering novelty (2018) IOP Conf. Series: *J. Phys.: Conf. Series*, 2019, 1198
doi:10.1088/1742-6596/1198/2/022074
15. Lauren, Botler; Nicholas, Jankowski; Patrick, McCluskey & Brian, Morgan. Numerical investigation and sensitivity analysis of manifold microchannel coolers. *Int. J. of Heat and Mass Transfer*, 2012, **55**, 7698-7708,
doi: 10.1016/j.ijheatmasstransfer.2012.07.073
16. Yusnira, Husaini; Arnan, Mitchell; Gary, Rosengarten & Juliana, Johari. Manifold design for uniform fluid distribution in parallel microchannel, 2016. *IEEE 6th Int. Conf. Sys. Engg. Technol. (ICSET)* 2016, 57-60
17. Juan, Manuel García-Guendulain; José, Manuel Riesco-Avila; Francisco, Elizalde-Blancas; Juan, Manuel Belman-Flores & Juan, Serrano-Arellano. Numerical Study on the effect of distribution plates in the manifolds on the flow distribution and thermal performance of a flat plate solar collector. *Energ.*, 2018, **11**, 1-21.
doi:10.3390/en11051077
18. Liu, Hong & Li, Peiwen. Even distribution/ dividing of single-phase fluids by symmetric bifurcation of flow channels. *Int. J. heat and fluid flow*, 2013, **40**, 165-179
doi: 10.1016/j.ihheatfluidflow.2013.01.011
19. Wang, Junye. Theory of flow distribution in manifolds. *Chemical Engineering Journal*, 2011, **168**, 1331-1345
doi: 10.1016/j.cej.2011.02.050
20. Wang, Junye & Wang, Hualin. Discrete method for design of flow distribution in manifolds. *Appl. Therm. Engg.*, 2015, **89**, 927-945
doi: 10.1016/j.applthermaleng.2015.06.069
21. Tomor, Andras & Kristof, Gergely. Validation of a discrete model for flow distribution in dividing-flow manifolds: Numerical and experimental studies. *Periodica Polytechnica Mech. Engg.*, 2016, **60**(1), 41-49
doi: 10.3311/PPme.8518
22. Wei, Min; Fan, Yilin; Luo, Lingai & Gilles Flamant. CFD-based evolutionary algorithm for the realization of target fluid flow distribution among parallel channels. *Chemical Engineering Research and Design*, 2015, **100**, 341-352
doi: 10.1016/j.cherd.2015.05.031
23. Wei, Min; Boutin, Guillaume; Fan, Yilin & Luo, Lingai. Flamant numerical and experimental investigation on the realization of target flow distribution among parallel mini-channels. *Chem. Engg. Res. Design*, Elsevier, 2016, **113**, 74-84
doi: 10.1016/j.cherd.2016.06.026.
24. Zeng, Shi & Lee, Poh Seng. A Header Design Method for Target Flow Distribution among Parallel Channels Based on Topology Optimization. *17th IEEE ITherm Conference* 156-164
25. Design of Experiments©, 1999-2019 Paul Mathews
26. Seok, Woochan; Kim, Gwan Hoon; Seo, Jeonghwa & Rhee, Shin Hyung. Application of the Design of Experiments and Computational Fluid Dynamics to Bow Design Improvement. *J. Marine Sci. Engg.*, 2019, **7**, 226
doi: 10.3390/jmse7070226
27. Aji, Mathew Abraham & Sadasivan, Anil Lal. Optimisation of a draft tube using surrogate modeling and genetic Algorithm. *J. Institution of Engg. (India) Series C102*, 2021, **3**, 753-764
doi: 10.1007/s40032-021-00674-y
28. Wang, Gary. Review of metamodeling techniques in support of engineering design optimization. *J. Mech. Design*, 2007, **129**(4), 370-380
doi: 10.1115/1.2429697
29. Yondo, Raul; Andres, Esther & Valero, Eusebio. A review on design of experiments and surrogate models in aircraft real-time and many-query aerodynamic analyses. *Progress in AeroSci.*, 2018, **96**, 23–61
doi: 10.1016/j.paerosci.2017.11.003

CONTRIBUTORS

Ms S. Annapurna, received her BTech (Mechanical Engineering) in 1995 and MTech (Heat Power-Refrigeration & Air Conditioning) in 2004 from J.N.T.U. College of Engineering, Anantapur, Andhra

Pradesh. Presently, she is working as a Scientist at DRDO, Centre for Air Borne Systems, Bangalore. Her areas of interest are: Electronics cooling, thermal design, and analysis.

Her contributions to the present work are: Conceptualization of problem, literature survey, carrying numerical simulations, and writing manuscript.

Ms Suma Varughese has joined DRDO in 1989. She received her MS (Engineering) in 2000 from the Indian Institute of Science, Bangalore. She is presently the Director-General for Medium Electronic Devices and Computational Systems, DRDO.

Her contributions to the present work involve reviewing the analysis and results.

Dr A.C. Niranjappa obtained his PhD from the Indian Institute of Science, Bangalore. Presently, he is working as an Outstanding

Scientist at DRDO, Centre for Air Borne Systems, Bangalore. He has published several technical articles. He has expertise in composite radome.

His contribution to the present work is analysing the simulations results and editing the manuscript.

Prof. K. Hema Chandra Reddy is a professor in Mechanical Engineering at JNTU College of Engineering, Ananatapuramu. Currently, he is serving as the Chairman of the Andhra Pradesh State Council of Higher Education. He has more than 30 years of teaching & research experience in the field of Mechanical Engineering, specialized in the areas of thermal engineering, CFD. He has published 135 technical papers in various national and international journals. His contribution to the present work is overall guidance to the problem approach.